PCCP

PAPER

The $K_2(9\text{-ethylguanine})_{12}^{2+}$ quadruplex is more stable to unimolecular dissociation than the $K(9\text{-ethylguanine})_8^+$ quadruplex in the gas phase: A BIRD, Energy Resolved SORI-CID, IRMPD Spectroscopic, and Computational Study

Received 00th January 20xx,
Accepted 00th January 20xx

DOI: 10.1039/x0xx00000x

Mohammad Azargun,[a] Paul Meister,[b] James W. Gauld,[b] and Travis D. Fridgen [a,*]

A combination of experimental trapped-ion mass spectrometric studies and computational chemistry has been used in the present work to assess the intrinsic properties of the potassiated 9-ethylguanine (9eG) self-assembled quadruplex, $K_2(9eG)_{12}^{2+}$, in the gas phase. Infrared multiple photon dissociation (IRMPD) spectroscopy in the N-H/C-H stretching region (2700 – 3800 cm^{-1}) revealed that this G-quadruplex is a sandwich-type structure with two G-tetrads sandwiching each of the two K^+, very similar to the structure determined previously for the $K(9eG)_8^+$ complexes. The stability of $K_2(9eG)_{12}^{2+}$ toward unimolecular dissociation and its binding energy were examined using energy-resolved sustained off-resonance collision induced dissociation (SORI-CID) and blackbody infrared radiative dissociation (BIRD) kinetics experiments. SORI-CID experiments showed that the self-assembled $K_2(9eG)_{12}^{2+}$ complex undergoes charge separation forming $K(9eG)_8^+$ and $K(9eG)_4^+$ compared to $K(9eG)_8^+$ which loses neutral 9eG. More interestingly, $K_2(9eG)_{12}^{2+}$ is more stable toward unimolecular dissociation activated by SORI-CID than the $K(9eG)_8^+$ complex. Temperature dependent BIRD kinetics for $K_2(9eG)_{12}^{2+}$ were consistent with energy-resolved SORI-CID results showing that $K_2(9eG)_{12}^{2+}$ to have an activation energy of 225±15 kJ mol^{-1}, approximately 50 kJ mol^{-1} greater than that determined for $K(9eG)_8^+$. The extra stability of $K_2(9eG)_{12}^{2+}$ is apparently not thermodynamic stability, but most likely due to an energy barrier for dissociation.

1. Introduction

G-tetrads and G-quadruplexes, Scheme 1A and 1B, are secondary structures of DNA that can be adopted in guanine-rich sequences of DNA and RNA.[1-6] Formation of thermodynamically stable G-tetrads is kinetically fast[7] and assisted by the unique locations of hydrogen bond donating and accepting groups in the guanine nucleobase. Metal cations are shown to stabilize and facilitate the formation of G-tetrads by neutralizing the excess negative potential from the four carbonyl oxygens of guanine molecules.[8, 9] Four-stranded G-quadruplexes can readily form by the self-stacking of planar G-tetrads with a metal cation between each layer (see Scheme 1 B).[10-14]

G-quadruplexes were first observed in the telomere region– the ends of chromosomes which cap and preserve DNA from degradation and reaction with other DNA molecules.[15, 16] DNA loses some of its telomeric region during mitotic cycles. This shortening of the telomere region has been understood to play an important role in the aging process;[17-19] once the telomere reaches its critical length, the cell dies. Telomeric G-quadruplexes not only contribute to the aging process, but it has also been shown to have potential for anti-cancer strategies.[20-22] Telomeric quadruplexes have been shown to induce cellular senescence in cancer cells by inhibiting telomerase activity, responsible for the elongation of the telomeric region.[23] As a result, stabilization of telomeric G-quadruplexes by small ligands has presented promising results toward treatment of a variety of cancers.[24-26]

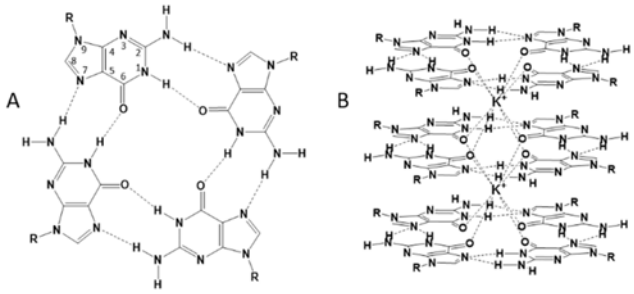

Scheme 1. Structures of A) G-tetrad and B) K^+ stabilized G-quadruplex. The 9-position is indicated by the R group.

The biological importance of G-quadruplexes has been greatly increased by their observation in regions of the DNA molecule other than the telomeric region.[27-33] Tetrad sequences have been traced in the first intron, first exon, promoter, and 5'-untranslated regions (5'-UTRs). Work conducted by Hurley and coworkers[33] has proposed the presence of a G-quadruplex at the promoter region of c-Myc gene, an essential activator in the expression and regulation of many genes. It was shown that this G-quadruplex can function as a transcriptional suppressor in order to control the transcription of c-Myc gene. The inhibitory role of guanine quadruplexes has been incorporated in methods which use small molecules to induce formation of

[a] Department of Chemistry, Memorial University of Newfoundland, St. John's, NL, Canada.
[b] Department of Chemistry and Biochemistry, University of Windsor, Windsor, ON, Canada.
*tfridgen@mun.ca.
Electronic Supplementary Information (ESI) available: [details of any supplementary information available should be included here]. See DOI: 10.1039/x0xx00000x

Please do not adjust margins

quadruplexes in the promoter region of oncogenes—genes with potential to cause cancer.[34] G-quadruplexes have found numerous therapeutic applications mainly as targets to land drugs and manipulate the gene activity of diseased and cancerous cells. Work performed by Leonetti *et al*.[35] selectively targeted DNA G-quadruplexes by an organic ligand, EMICRON; $C_{52}H_{59}N_6O_4{\cdot}4HCl$. The resulting complex showed great damage to telomeres in cancer cells, and cell proliferation in tumour cells was observed to be greatly suppressed. Due to their affinity for self-assembly into supramolecular scaffolds, G4s have also received much attention in materials science, nanotechnology, and sensor designing.[3, 36-43]

The effect of biologically relevant ions including Na^+ and K^+ on the formation and stability of guanine tetrads has also been investigated in the gas phase.[44] Infrared multiphoton dissociation (IRMPD) spectroscopy and energy-resolved collision induced dissociation (CID) studies of $M(9eG)_4^+$ complexes (9eG = 9-ethylguanine, M = alkali metal, see Scheme 1) have revealed that Na^+ forms the most strongly bound gas-phase G-tetrad, followed by Li^+, then K^+, Rb^+, and Cs^+. This conclusion was in agreement with experiments probing the solution phase stabilities conducted by Fukushima and coworkers.[45] It has also been shown, spectroscopically and computationally, that $Na(9eG)_4^+$ adopts a square planar structure[44, 46] with Na^+ at the centre, while other larger metals such as K^+, Rb^+ and Cs^+ sit above the plane formed by four guanine molecules.[44] The observed stability trend, $Na^+ >> Li^+ > K^+ > Rb^+ > Cs^+$, is not entirely consistent with what is expected based on purely electrostatic grounds under which Li^+ would have the strongest interaction with guanine molecules.[47, 48] Calculations showed that Li^+ strongly distorts the planar hydrogen bonded structure, but while Na^+ also distorts the tetrad structure, it preserves the planarity and hydrogen bonding network; it is the extra distortion of the tetrad by Li^+ that makes $Li(9eG)^+$ less stable to dissociation than $Na(9eG)^+$.[44]

The chemistry of the G-quadruplex clusters composed of two or more G-tetrads has also been the subject of both solution and gas phase studies. Proton NMR chemical shift studies[49] examined the competition between K^+ and Na^+ for coordination to G-tetrads. In this regard, the oligonucleotide $d(G_3T_4G_3)$ was exposed to metal chloride (NaCl and KCl) solutions. It was reported that two Na^+ cations in the G-quadruplex composed of three G-tetrads are displaced by two K^+, a thermodynamically favourable process, $(\Delta_rG°) = -7.11 \pm 0.15$ kJmol^{-1}. It was also suggested that the replacement of Na^+ is not necessarily the result of an optimal fit of K^+ in the G-tetrad cavities, but it is due to the larger hydration energy of Na^+. This conclusion was also supported by computational work[50] proposing that although the cage formed by the sandwiching tetrads acts as a better host for K^+, still the process is governed by relative hydration energies. However, it is important to point out that in gas phase studies—in the absence of solvent—K^+ quadruplexes composed of two 9-ethylguanine tetrads were determined to be significantly more thermodynamically stable than those composed of Na^+.[51]

The results of an equilibrium titration study[52] showed that quadruplexes form through intermediates composed of G-tetrads stabilized by metal cations with further strand rearrangements to yield the quadruplex. It was also suggested that the formation of quadruplexes stabilized by K^+ is less complex than processes resulting in Na^+ stabilized G-quadruplexes. This observation is consistent with our previous gas phase studies[51] showing that decomposition of the Na^+-stabilized quadruplex occurred by losing one guanine at a time while K^+ stabilized quadruplexes lose a neutral G-tetrad in a single step.

In the present work, the gas phase, self-assembled $K_2(9eG)_{12}^{2+}$ (9eG=9-ethylguanine) complex has been studied for the first-time using ion-activation techniques including blackbody infrared radiative dissociation (BIRD), sustained off-resonance irradiation collision induced dissociation (SORI-CID), and infrared multiple photon dissociation (IRMPD) spectroscopy.

2. Methods

2.1 Experimental

All experiments were conducted using a Bruker ApexQe 7.0 hybrid Fourier transform ion cyclotron resonance (FTICR) mass spectrometer in the Laboratory for the Study of the Energetics, Structures, and Reactions of Gaseous Ions at Memorial University.[53, 54] 9eG was purchased from Sigma-Aldrich and used without further purification. The solution was prepared by the addition of two drops of 1 mM KCl solution to 10 ml of 0.2 mM 9eG solution in 18 MΩ cm water. An Apollo II ion source coupled to the FTICR mass spectrometer was used to electrospray the solution at about 100 μL h^{-1}. SORI-CID experiments were carried out by isolating the G-quadruplex cluster inside the ICR cell (P = 10^{-10} mbar), exciting the ion by standard off-resonance irradiation techniques, while exposing the cluster ion to Ar inside the ICR cell at pressures of about 10^{-5} - 10^{-6} mbar. This pressure ensures 10's to 100's of collisions in a 250 ms excitation window. The average kinetic energies are expected to be 2/3 the maximum lab frame kinetic energies which are determined from Equation 1[55]

$$E_{\text{lab}}^{\max} = \frac{\beta^2 q^2 V_{p-p}}{32\pi^2 m d^2 \Delta\nu^2}$$

where β is a constant known as geometrical factor of the ICR cell (0.9 in the present case), q is the charge on the ion, $V_{p\text{-}p}$ is the peak to peak excitation voltage, m is the mass of the ion, d is the diameter of the ICR cell (6 cm), and $\Delta\nu$ is the frequency offset (500 Hz). The centre of mass (c.o.m.) ion kinetic energies for an individual collision can be obtained by a multiplication of the lab frame energies by.

$$m_{\text{Ar}} \Big/ \left(m_{\text{Ar}} + m_{quadruplex}\right).$$

An infrared (IR) optical parametric oscillator (OPO) (LaserSpec) tuneable from 2700 – 4000 cm^{-1} with a bandwidth of 2 cm^{-1}, was used to obtain IRMPD spectra. The OPO is built around a periodically poled lithium niobate crystal and is pumped by a diode-pumped, solid state, Nd:YAG laser. The OPO operates at 20 kHz, with a pulse duration of a few nanoseconds and generates output power near 1 W at 3 μm. A broad-band filter decreasing the maximum laser intensity to ~300 mW was used to avoid complete dissociation of the ions during resonant absorption. Following isolation of $K_2(9eG)_{12}^{2+}$ the laser was scanned at 2 cm^{-1} intervals and ions were irradiated for 1 s. The

 This journal is © The Royal Society of Chemistry 20xx

Please do not adjust margins

Please do not adjust margins

IRMPD efficiency is the negative logarithm of the ratio of the precursor ion intensity divided by the total ion intensity.

For BIRD experiments, $K_2(9eG)_{12}^{2+}$ was isolated in the ICR cell with a background pressure of 10^{-10} mbar, and the precursor and product ion intensities were recorded after a varying period of reaction time at a specific temperature. BIRD kinetics were observed between 373 – 405 K. The BIRD rate constant (*k*) for each temperature was determined by fitting the experimental quadruplex intensity vs time plots to the integrated first order rate law,

$$[I]_t = e^{-kt}$$

in which $[I]_t$ is the normalized intensity of the quadruplex at reaction time, *t*. A plot of the BIRD rate constants as a function of the inverse temperature was used to determine the Arrhenius pre-exponential factor (A^{obs}) and activation energy (E_a^{obs}) from the intercept and slope, respectively according to the Arrhenius equation:

$$\ln k = \ln A_{obs} - \frac{E_{a,obs}}{k_B T}$$

2.2. Computational

All calculations were performed using the Gaussian 16 program. Optimized geometries and harmonic frequencies were obtained using a variety of hybrid, meta-hybrid, and range-separated density functionals (B3LYP,[56, 57] PBE0,[58] M06-2X,[59] and ωB9X-D[60]) with a systematic series of basis sets (6-311G(d,p), 6-311+G(d,p), 6-311+G(2d,p), 6-311+G(df,p), 6-311+G(2d,2p), and 6-311+G(2df,p)). It is noted that we previously used the B3LYP method to examine changes in guanine quartets induced by protonation.[61] Herein, we considered the ability of a broader variety of functionals. The frequency calculations confirmed all structures were energy minima. For the quartets, 9-methylguanine (9mG) was used rather than the ethyl derivative 9eG and structures were obtained for $(9mG)_4$, $K(9mG)_4^+$, $(9mG)_8$, $K(9mG)_8^+$, $(9mG)_{12}$, $K(9mG)_{12}^+$, and $K_2(9mG)_{12}^{2+}$.

3. Results and Discussion

In the present work, 9eG was used instead of guanine for two reasons—9eG is more soluble than guanine and N9 is blocked by an ethyl group eliminating the possibility of interaction between K^+ and 9eG through N9. This N9 blockage makes the 9eG a better model for biological systems since N9 is the site of attachment to the phosphate backbone in DNA and RNA bases. The sugar-phosphate backbone has been shown to play an insignificant role in the affinity of metal cations to the quadruplexes and also their stabilities.[62-65] The focus of the present study is a simplified G-quadruplex system composed of three G-tetrads in the absence of the sugar-phosphate backbone, to probe the intrinsic physical chemistry of the gas-phase quadruplex.

Figure S1 depicts an electrospray mass spectrum of 9-ethylguanine/KCl aqueous solution. $K(9eG)_4^+$, $K(9eG)_8^+$, and $K_2(9eG)_{12}^{2+}$ are present, each being made of multiples of four 9-ethylguanines, the G-tetrad building block. Note that the very very stable $Na(9eG)_4^+$ was also observed even though no Na^+ was added to the solution. The structure and stability of $K(9eG)_4^+$ and $K(9eG)_8^+$ to loss of 9eG and $(9eG)_4$, respectively, were discussed in previous communications.[44,51] It was shown that among the, $M(9eG)_8^+$ (where M=Na, K, Rb, Cs), $K(9eG)_8^+$ is the most stable while among $M(9eG)_4^+$ (where M=Li, Na, K, Rb, Cs) the planar $Na(9eG)_4^+$ was the most strongly bound G-tetrad.[44,51] Interestingly, $K_2(9eG)_{12}^{2+}$ was the largest G-quadruplex generated which is consistent with most G-quadruplexes found in the biological systems which are formed by three tetrads and two potassium cations.[66-68]

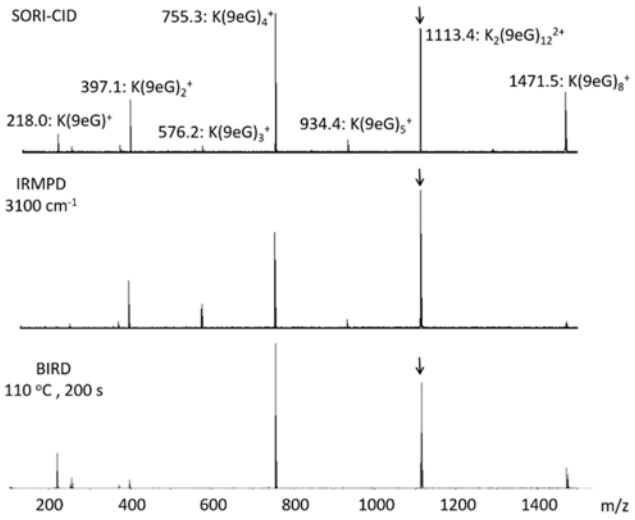

Figure 1. FTICR mass spectra recorded following SORI-CID with c.o.m. collision energy of 0.30 eV (top), IRMPD for 1 s with OPO(A) radiation at 3100 cm^{-1} (middle), and 200 s of BIRD at 110 °C (bottom) of isolated $K_2(9eG)_{12}^{2+}$, *m/z* 1113.4 (indicated by the arrow in each experiment).

3.1 Unimolecular Dissociation. Figure 1 shows the results of activation of $K(9eG)_{12}^{2+}$ conducted by using SORI-CID, IRMPD, and BIRD. In all cases the main dissociation channel for $K(9eG)_{12}^{2+}$ is charge separation forming $K(9eG)_4^+$ and $K(9eG)_8^+$ at *m/z* 1471.5 and 755.3, respectively. The SORI-CID and IRMPD mass spectra look similar with some other fragmentation products such as $K(9eG)_5^+$, $K(9eG)_3^+$, $K(9eG)_2^+$, and $K(9eG)^+$ also present. BIRD is a relatively soft activation technique compared to CID and IRMPD and produces a simpler spectrum with only $K(9eG)_2^+$ and $K(9eG)^+$ observed besides the precursor and main charge separation products.

It is interesting to note that the intensity of $K(9eG)_8^+$ in all three mass spectra is much less than the $K(9eG)_4^+$. Based on the stoichiometry of this fragmentation reaction, the intensities of these two ions should be the same. However, $K(9eG)_8^+$ also dissociates to lose a neutral tetrad as observed previously.[51] The disparity between the $K(9eG)_4^+$ and $K(9eG)_8^+$ intensities is most pronounced for the IRMPD and BIRD activation techniques since all precursor and fragment ions are continuously absorbing radiation during activation and $K(9eG)_8^+$ has a higher BIRD rate constant than $K_2(9eG)_{12}^{2+}$ (*vide infra*). This is different than in CID where activation is of $K_2(9eG)_{12}^+$ exclusively, with any secondary dissociation of the fragment ions being due to excess internal energy partitioned to those fragments during activation of the precursor. This can be seen in Figure S2 where the $K(9eG)_8^+$ and $K(9eG)_4^+$ have *more* similar intensities up to about 0.20 eV where energy is deposited into the precursor ion faster and some of the excess energy is partitioned to products. Note though, that the $K(9eG)_4^+$ intensity is greater than that of $K(9eG)_8^+$ at all collision energies observed. We will have more to say about this below. That $K(9eG)_4^+$ his significantly higher in intensity than the $K(9eG)_8^+$ cluster under BIRD and IRMPD

Please do not adjust margins

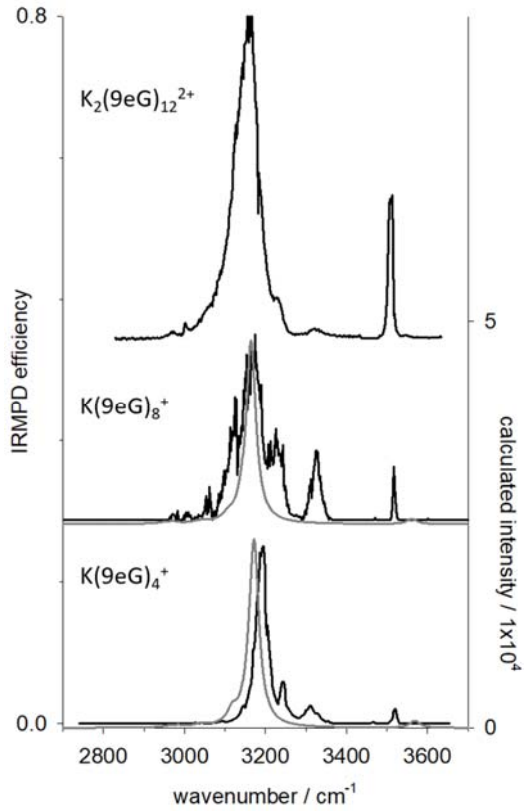

Figure 2. IRMPD spectra of the potassiated tetrad and quadruplexes. The grey traces are computed IR spectra at the B3LYP/SVP level of theory. The $K(9eG)_8^+$ and $K(9eG)_4^+$ spectra were reported in references 51 and 44, respectively.

conditions is because the latter dissociates readily losing a $(9eG)_4$ tetrad forming more $K(9eG)_4^+$.

3.2. IRMPD Spectroscopy $K_2(9eG)_{12}^{2+}$. In Figure 2 the IRMPD spectrum of $K_2(9eG)_{12}^{2+}$ is compared to those of the $K(9eG)_8^+$ and $K(9eG)_4^+$ clusters in the 2700 – 3800 cm^{-1} region. It is apparent that all clusters show similar spectral features containing a broad feature centred at about 3160 cm^{-1} attributed to hydrogen bonded N-H stretching modes. There is also a feature just above 3500 cm^{-1} attributed to free N-H stretching, respectively.[44,46,51] The feature observed at about 3320 cm^{-1} has been assigned to the C=O stretching overtone.[44,46]

In our previous work, it was shown by IRMPD spectroscopy and computational chemistry that $M(9eG)_4^+$ clusters (M= Li, Na, K, Rb and Cs) form similar structures with Hoogsteen base pairing in which metals occupy the cavity (Scheme 1). It was observed that $M(9eG)_4^+$ clusters were indistinguishable using IRMPD spectroscopy. In addition, IRMPD spectroscopy on $M(9eG)_8^+$ (M= Na, K, Rb, and Cs) clusters resulted in the same conclusion. The $M(9eG)_8^+$ experimental IRMPD spectra displayed very similar features which were interpreted to conclude that these clusters exist in a sandwich structure with a metal cation between two G-tetrads. Computational studies in conjunction with the vibrational spectra were used to rule out the co-existence of non-sandwich structures. Figure 2 shows that the larger G-quadruplex, $K(9eG)_{12}^{2+}$, presents a very similar spectrum compared to $K(9eG)_8^+$ and $K(9eG)_4^+$. It is concluded

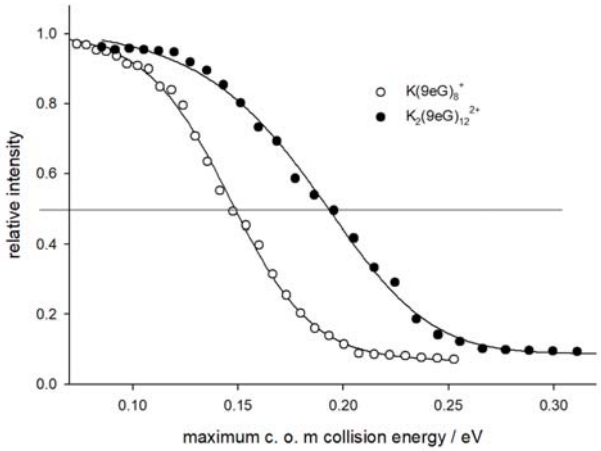

Figure 3. Precursor ion intensity vs. the centre of mass (c.o.m.) collision energy decay curves for $K(9eG)_8^+$ and $K_2(9eG)_{12}^{2+}$ From SORI-CID mass spectrometry experiments. The reservoir pressure was 10 mbar in Ar. The higher energy required to dissociate $K_2(9eG)_{12}^{2+}$ indicates that it is more stable to dissociation than $K(9eG)_8^+$.

that $K(9eG)_{12}^{2+}$ also adopts a sandwich structure in which three G-tetrads are stacked with K^+ between each pair of tetrads.

3.3 Energy-Resolved SORI-CID. Energy-resolved SORI-CID was used to probe the relative gas phase stabilities of potassium the quadruplexes $K_2(9eG)_{12}^{2+}$ and $K(9eG)_8^+$. Clusters were isolated and then excited to collision energies of between 0 and 0.35 eV in the centre of mass frame and then exposed to Ar gas with a reservoir pressure of 10 mbar Ar. The energy resolved breakdown curves for $K_2(9eG)_{12}^{2+}$ and its products are depicted in Figure S2. The $K_2(9eG)_{12}^{2+}$ quadruplex undergoes charge separation into two singly charged ions, $K(9eG)_4^+$ and $K(9eG)_8^+$. Furthermore, $K(9eG)_8^+$ from $K_2(9eG)_{12}^{2+}$ loses a neutral tetramer, as was previously observed,[51] to also form $K(9eG)_4^+$. Only small amounts of product ions other than $K(9eG)_4^+$ and $K(9eG)_8^+$ were observed showing that these clusters primarily dissociate by losing a G-tetrad unit.

Figure 3 depicts plots of the normalized intensities of precursor $K(9eG)_8^+$ and $K_2(9eG)_{12}^{2+}$ quadruplexes against the centre of mass collision energy from two different experiments beginning with either isolated $K(9eG)_8^+$ or $K_2(9eG)_{12}^{2+}$. It is clear that $K(9eG)_8^+$ dissociates at lower centre of mass collision energies than that required for $K_2(9eG)_{12}^{2+}$; a line is drawn to mark the 50% dissociation of clusters to make this clear. $K_2(9eG)_{12}^{2+}$ is more stable to collision induced dissociation compared to the smaller singly charged quadruplex, $K(9eG)_8^+$.

3.4 BIRD experiments. Temperature dependent rate constants were determined for unimolecular dissociation of the G-quadruplexes bathing in the ambient blackbody radiation of the ICR cell. Figure S3 shows a breakdown diagram for the $K_2(9eG)_{12}^{2+}$ under BIRD conditions at 385 K. In Figure 4 the Arrhenius plots are compared for BIRD of $K_2(9eG)_{12}^{2+}$ from this work and that of $K(9eG)_8^+$ from previous work.[51] The Corresponding observed activation energies (E_0) and log A^{obs} are summarized in Table 1. It is worth noting that the ratio of the activation energies for $K_2(9eG)_{12}^{2+}$ and $K(9eG)_8^+$ is 1.3, similar to the ratio of the 50% ER-CID values in Figure 3.

Note that the BIRD rate constants for both quadruplexes are in the rapid exchange limit which is the case for large, slowly

This journal is © The Royal Society of Chemistry 20xx

Table 1. Observed activation energies, preexponential factors and the entropy of activation for $K_2(9eG)_{12}^{2+}$ and $K(9eG)_8^+$.

Species	E_a^{obs} / kJ mol^{-1}	Log A^{obs}	$\Delta S^{\dagger}$ / J K^{-1} mol^{-1}
$K_2(9eG)_{12}^{2+}$	225±15	28.2	286±20
$K(9eG)_8^+$	176±11	21.9	166±11

dissociating ions such that the ions are in thermal equilibrium with the surroundings. This was confirmed for $K(9eG)_8^+$ where master equation modelling reproduced the observed activation energy.[51]

The Arrhenius activation energy for $K_2(9eG)_{12}^{2+}$ was determined to be 225 kJ mol^{-1}; 49 kJ mol^{-1} higher than the value observed for $K(9eG)_8^+$. This agrees with the results of the SORI-CID experiments presented in the previous section where a higher centre of mass energy was required to dissociate $K_2(9eG)_{12}^{2+}$ than $K(9eG)_8^+$.

Computed binding energies of $K(9eG)_8^+$ and $K_2(9eG)_{12}^{2+}$ are presented in Table 2. The binding energies for $K(9eG)_8^+$ are in general agreement with the experimental value of 176 kJ mol^{-1}, although the wB97XD predict a binding energy almost 100 kJ mol^{-1} higher, and the PBE0 calculations making the best estimate of the experimental value. For the $K_2(9eG)_{12}^{2+}$ quadruplex, both the B3LYP and PBE0 calculations predict the binding energy to be negative, meaning it is thermodynamically unbound at those levels of theory. In all four cases the binding energy for $K_2(9eG)_{12}^{2+}$ is predicted to be significantly lower than that for $K(9eG)_8^+$. This means the extra stability observed independently in the energy-resolved SORI-CID and temperature-dependent BIRD experiments may not be a thermodynamic stability, but a kinetic stability.

Doubly-charged ions in the gas phase are typically stabilized by a large activation energy which manifests itself in large kinetic energy releases observed for their dissociation in double focussing mass spectrometers.[69] To account for these large activation energies in the dissociation of multiply charged ions, an avoided crossing between two diabatic potentials—one for loss of a neutral fragment and one for the charge separation—such as the one in Figure 5 have been proposed.[70,71] In the present case, dissociation begins on the attractive part of the potential where neutral $K(9eG)_4$ begins to dissociate from the remaining $K(9eG)_8^{2+}$ dication. This is followed by an electron transfer from the neutral to the doubly charged cation which is lower in energy at infinite separation. This then leads to Coulomb repulsion between the two charged products, $K(9eG)_4^+$ and $K(9eG)_8^+$. In Table 2, the computed binding energies with respect to loss of neutral $K(9eG)_4$ are presented in the last column. As expected, the binding with respect to the neutral loss is quite high, ranging from over 500 to over 800 kJ mol^{-1}. A potential energy surface is sketched in Figure 5 based on the experimentally observed dissociation energy and the computed binding energies at the PBE0/6-311G(d,p) level and basis.

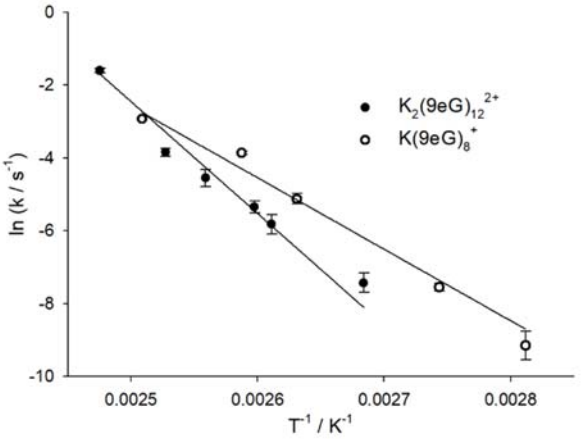

Figure 4. Arrhenius plots for the potassiated quadruplexes.

A large entropy of activation is determined from the BIRD experiments, 286±20 J K^{-1}, significantly higher than that observed for $K(9eG)_8^+$, 168 J K^{-1} mol^{-1}, which in itself is a value associated with a late transition state. This large entropy of activation is entirely consistent with the extremely late transition states that arise from avoided crossings. For the dissociation of multiply-charged fullerene ions,[72] the intercharge distances at the point of electron transfer, presumably the avoided crossing, were found to be between 70 and 80 nm. The added looseness of the entropy of activation in the present case may also be due to the weakly-bound nature

Table 2. Binding Energies (kJ mol^{-1}) for the potassiated quadruplexes.

Method and Basis	$K(9eG)_8^+$ Loss of $(9eG)_4$	$K_2(9eG)_{12}^{2+}$ Loss of $K(9eG)_4^+$	$K_2(9eG)_{12}^{2+}$ Loss of $K(9eG)_4$
B3LYP/			
6-311G(d,p)	144.9	-28.8	555.2
6-311+G(d,p)	122.0	-45.2	532.9
6-311+G(2d,p)	111.2	-53.3	523.6
6-311+G(df,p)	124.5	-45.0	534.6
6-311+G(2d,2p)	111.3	-53.9	522.8
6-311+G(2df,p)	112.7	-54.3	524.1
M062X/			
6-311G(d,p)	223.8	39.4	732.9
6-311+G(d,p)	217.0	29.8	716.6
6-311+G(2d,p)	201.0	17.6	702.5
6-311+G(df,p)	220.7	30.6	
6-311+G(2d,2p)	199.7	16.6	701.4
6-311+G(2df,p)	204.0	17.7	704.5
wB97XD/			
6-311G(d,p)	275.1	103.1	822.0
6-311+G(d,p)	264.3	94.3	816.0
6-311+G(2d,p)	251.7	84.8	805.2
6-311+G(df,p)	266.7	94.2	816.7
6-311+G(2d,2p)	251.5	84.2	
6-311+G(2df,p)	253.4	83.9	
PBE0/			
6-311G(d,p)	166.5	-7.4	596.5
6-311+G(d,p)	154.6	-13.8	584.7
6-311+G(2d,p)	140.8	-24.5	572.7
6-311+G(df,p)	157.2	-13.5	586.3
6-311+G(2d,2p)	140.8	-25.0	571.9

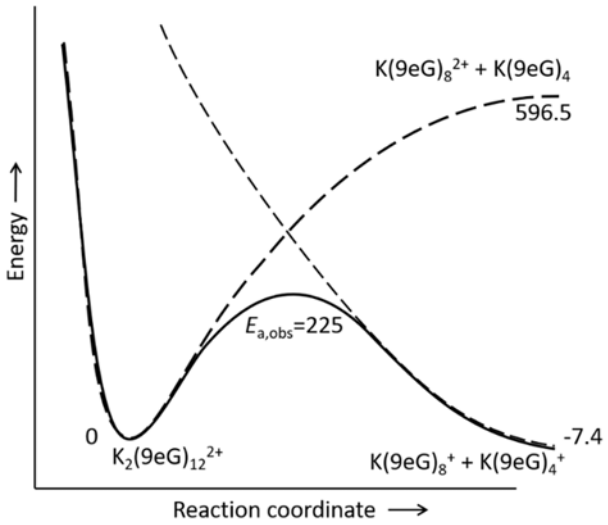

Figure 2. Schematic representation of the origin of the kinetic barrier to the charge separation reaction of $K_2(9eG)_{12}^{2+}$. An avoided crossing between diabatic potential energy surfaces (dashed lines) results in the adiabatic potential energy surface (solid line).

of the $K(9eG)_4$ moiety of the transition state which, due to being neutral, the bases would be less tightly bound to the metal and the inter-complex hydrogen bonds would also be weaker without the positive charge.

Conclusions

The present study is the first investigation into the charge separation decomposition of a model guanine quadruplex. Both energy-resolved SORI-CID and BIRD experiments showed that the $K_2(9eG)_{12}^{2+}$ dissociation into $K(9eG)_8^+$ and $K(9eG)_4^+$ has a higher energy requirement than the loss of a neutral guanine tetrad from $K(9eG)_8^+$. Calculations show that the dissociation of $K_2(9eG)_{12}^{2+}$ is thermodynamically preferred over the $K(9eG)_8^+$ dissociation. It is concluded that the stability of $K_2(9eG)_{12}^{2+}$ is due to a large barrier to its dissociation due to an avoided crossing that is inherent in charge separation reactions.

Conflicts of interest

There are no conflicts to declare.

Acknowledgements

Financial support of this work from the Natural Sciences and Engineering Research Council (NSERC) of Canada (J.W.G., T.D.F.) is gratefully acknowledged. The Canada Foundation for Innovation (CFI), The Industrial Research and Innovation Fund (IRIF), and Bruker are gratefully acknowledged for their support for the Laboratory for the Study of Gaseous Ion Structures, Energetics and Reactions (T.D.F.). Computational support from Compute Canada are also gratefully acknowledged. A referee is sincerely thanked for their thorough review and for several very insightful suggestions.

Notes and references

1. S. Burge, G. N. Parkinson, P. Hazel, A. K. Todd and S. Neidle, *Nucleic Acids Res.*, 2006, **34**, 5402-5415.
2. A. T. Phan, V. Kuryavyi and D. J. Patel, *CURR OPIN STRUC BIOL*, 2006, **16**, 288-298.
3. J. T. Davis, *Angew. Chem. Int. Ed.*, 2004, **43**, 668-698.
4. T. Simonsson, *Biol. Chem.* , 2001, **382**, 621-628.
5. R. Hänsel-Hertsch, J. Spiegel, G. Marsico, D. Tannahill and S. Balasubramanian, *Nat. Protoc.*, 2018, **13**, 551.
6. O. Mendoza, A. Bourdoncle, J.-B. Boulé, J. R. M. Brosh and J.-L. Mergny, *Nucleic Acids Res.*, 2016, **44**, 1989-2006.
7. A. N. Lane, J. B. Chaires, R. D. Gray and J. O. Trent, *Nucleic Acids Research*, 2008, **36**, 5482-5515.
8. N. H. Campbell and S. Neidle, in *Interplay between Metal Ions and Nucleic Acids*, Springer, 2012, pp. 119-134.
9. S. N. Georgiades, N. H. Abd Karim, K. Suntharalingam and R. Vilar, *Angew. Chem. Int. Ed.*, 2010, **49**, 4020-4034.
10. D. J. Patel, A. T. Phan and V. Kuryavyi, *Nucleic Acids Res.*, 2007, **35**, 7429-7455.
11. S. Neidle and S. Balasubramanian, in *Quadruplex Nucleic Acids*, The Royal Society of Chemistry, 2006, DOI: 10.1039/9781847555298-00001, pp. 1-30.
12. J. Dai, M. Carver and D. Yang, *Biochimie*, 2008, **90**, 1172-1183.
13. G. Wu, A. Wong, Z. Gan and J. T. Davis, *J. Am. Chem. Soc.*, 2003, **125**, 7182-7183.
14. S. Nagatoishi, T. Nojima, B. Juskowiak and S. Takenaka, *Angew. Chem. Int. Ed.*, 2005, **117**, 5195-5198.
15. G. N. Parkinson, M. P. Lee and S. Neidle, *Nature*, 2002, **417**, 876-880.
16. Y. Wang and D. J. Patel, *Structure*, 1993, **1**, 263-282.
17. C. B. Harley, *Cold Spring Harbor Monograph Archive*, 1995, **29**, 247-263.
18. C. B. Harley, H. Vaziri, C. M. Counter and R. C. Allsopp, *Exp. Gerontol.*, 1992, **27**, 375-382.
19. G. Aubert and P. M. Lansdorp, *Physiol. Rev.*, 2008, **88**, 557-579.
20. G. W. Collie, R. Promontorio, S. M. Hampel, M. Micco, S. Neidle and G. N. Parkinson, *J. Am. Chem. Soc.*, 2012, **134**, 2723-2731.
21. L. Oganesian and T. M. Bryan, *BioEssays*, 2007, **29**, 155-165.
22. S. Neidle, *FEBS J.*, 2010, **277**, 1118-1125.
23. G. Pennarun, C. Granotier, L. R. Gauthier, D. Gomez, F. Hoffschir, E. Mandine, J.-F. Riou, J.-L. Mergny, P. Mailliet and F. D. Boussin, *Oncogene*, 2005, **24**, 2917-2928.
24. G. W. Collie, S. M. Haider, S. Neidle and G. N. Parkinson, *Nucleic acids research*, 2010, gkq259.
25. G. Collie, A. P. Reszka, S. M. Haider, V. Gabelica, G. N. Parkinson and S. Neidle, *Chem. Commun.*, 2009, 7482-7484.
26. D. Drygin, A. Lin, J. Bliesath, C. B. Ho, S. E. O'Brien, C. Proffitt, M. Omori, M. Haddach, M. K. Schwaebe and A. Siddiqui-Jain, *Cancer Res.*, 2011, **71**, 1418-1430.
27. A. Arora, M. Dutkiewicz, V. Scaria, M. Hariharan, S. Maiti and J. Kurreck, *RNA*, 2008, **14**, 1290-1296.
28. R. Shahid, A. Bugaut and S. Balasubramanian, *Biochemistry*, 2010, **49**, 8300-8306.
29. G. D. Balkwill, K. Derecka, T. P. Garner, C. Hodgman, A. P. F. Flint and M. S. Searle, *Biochemistry*, 2009, **48**, 11487-11495.
30. J. L. Huppert and S. Balasubramanian, *Nucleic Acids Res.*, 2007, **35**, 406-413.
31. Y. Qin and L. H. Hurley, *Biochimie*, 2008, **90**, 1149-1171.
32. Y. Wu and R. M. Brosh, *FEBS J.*, 2010, **277**, 3470-3488.
33. A. Siddiqui-Jain, C. L. Grand, D. J. Bearss and L. H. Hurley, *Proc. Natl. Acad. Sci.* , 2002, **99**, 11593-11598.
34. A. Rangan, O. Y. Fedoroff and L. H. Hurley, *J. Biol. Chem.*, 2001, **276**, 4640-4646.
35. M. Porru, S. Artuso, E. Salvati, A. Bianco, M. Franceschin, M. G. Diodoro, D. Passeri, A. Orlandi, F. Savorani and M. D'Incalci, *Mol. Cancer Ther.*, 2015, **14**, 2541-2551.
36. I. German, D. D. Buchanan and R. T. Kennedy, *Anal. Chem.*, 1998, **70**, 4540-4545.
37. R. Nutiu and Y. Li, *J. Am. Chem. Soc.*, 2003, **125**, 4771-4778.
38. H. Ueyama, M. Takagi and S. Takenaka, *J. Am. Chem. Soc.*, 2002, **124**, 14286-14287.
39. T. C. Marsh and E. Henderson, *Biochemistry*, 1994, **33**, 10718-10724.
40. T. C. Marsh, J. Vesenka and E. Henderson, *Nucleic Acids Res.*, 1995, **23**, 696-700.
41. T.-Y. Dai, S. P. Marotta and R. D. Sheardy, *Biochemistry*, 1995, **34**, 3655-3662.
42. R. B. Kotia, L. Li and L. B. McGown, *Anal. Chem.*, 2000, **72**, 827-831.
43. J. T. Davis and G. P. Spada, *Chem. Soc. Rev.*, 2007, **36**, 296-313.
44. M. Azargun and T. D. Fridgen, *Phys. Chem. Chem. Phys.*, 2015, **17**, 25778-25785.
45. K. Fukushima and H. Iwahashi, *Chem. Commun.*, 2000, 895-896.
46. C. Fraschetti, M. Montagna, L. Guarcini, L. Guidoni and A. Filippi, *Chem. Commun.*, 2014, **50**, 14767-14770.
47. M. T. Rodgers and P. B. Armentrout, *J. Am. Chem. Soc.*, 2000, **122**, 8548-8558.
48. B. A. Cerda and C. Wesdemiotis, *J. Am. Chem. Soc.*, 1996, **118**, 11884-11892.
49. N. V. Hud, F. W. Smith, F. A. Anet and J. Feigon, *Biochemistry*, 1996, **35**, 15383-15390.
50. F. R. Elder, A. M. Gurewitsch, R. V. Langmuir and H. C. Pollock, *Phys. Rev.*, 1947, **71**, 829-830.

This journal is © The Royal Society of Chemistry 20xx

Please do not adjust margins

51. M. Azargun, Y. Jami-Alahmadi and T. D. Fridgen, *Phys. Chem. Chem. Phys.*, 2017, **19**, 1281-1287.
52. R. D. Gray and J. B. Chaires, *Nucleic Acids Res.*, 2008, **36**, 4191-4203.
53. M. B. Burt and T. D. Fridgen, *Eur. J. Mass Spectrom*, 2012, **18**, 235-250.
54. T. D. Fridgen, *Mass Spectrom. Rev.*, 2009, **28**, 586-607.
55. C. Peltz, L. Drahos and K. Vékey, *J. Am. Soc. Mass Spectrom.*, 2007, **18**, 2119-2126.
56. Y. Zhao, N. E. Schultz and D. G. Truhlar, *J. Chem. Phys.*, 2005, **123**, 161103.
57. A. D. Becke, *J. Chem. Phys.*, 1993, **98**, 5648-5652.
58. C. Adamo and V. Barone, *J. Chem. Phys.*, 1999, **110**, 6158-6170.
59. Y. Zhao and D. G. Truhlar, *Theor. Chem. Acc*, 2008, **120**, 215-241.
60. J.-D. Chai and M. Head-Gordon, *Phys. Chem. Chem. Phys.*, 2008, **10**, 6615-6620.
61. H. Liu and J. W. Gauld, *Phys. Chem. Chem. Phys.*, 2009, **11**, 278-287.
62. J. R. Williamson, M. K. Raghuraman and T. R. Cech, *Cell*, **59**, 871-880.
63. W. I. Sundquist and A. Klug, *Nature*, 1989, **342**, 825-829.
64. F. Zaccaria, G. Paragi and C. Fonseca Guerra, *Phys. Chem. Chem. Phys.*, 2016, **18**, 20895-20904.
65. A. Wong and G. Wu, *J. Am. Chem. Soc.*, 2003, **125**, 13895-13905.
66. Y. Xu, *Chemical Society Reviews*, 2011, **40**, 2719-2740.
67. Y. Xu, K. Kaminaga and M. Komiyama, *J. Am. Chem. Soc.*, 2008, **130**, 11179-11184.
68. Y. Xu, Y. Suzuki, K. Ito and M. Komiyama, *Proc. Natl. Acad. Sci.*, 2010, **107**, 14579-14584.
69. J. Laskin and C. Lifshitz, *J. Mass Spectrom.*, 2001, **36**, 459-478.
70. P. M. W. Gill and L. Radom, *Chem. Phys. Lett.*, 1988, **147**, 213-218.
71. L. Radom, P. M. W. Gill, M. W. Wong and R. H. Nobes, *Pure Appl. Chem.*, 1988, **60**, 183.
72. P. Sceier, B. Dunser, T.D. Mark, J. Phys. Chem. 1995, 99, 15428-15437.

This journal is © The Royal Society of Chemistry 20xx

Please do not adjust margins